Korean J. Chem. Eng., **31**(1), 166-171 (2014)
DOI: 10.1007/s11814-013-0188-3

pISSN: 0256-1115
eISSN: 1975-7220

Microcellular foaming of silicone rubber with supercritical carbon dioxide

In-Kwon Hong and Sangmook Lee†

Department of Chemical Engineering, Dankook University, Gyeonggi 448-701, Korea
(*Received 10 June 2013 • accepted 26 September 2013*)

Abstract–In spite of great concern on the industrial application of microcellular silicone rubber foams, such as in electric and medical devices, only a few works can be found about the foaming of silicone rubber. In this study, microcellular silicone rubber foams with a cell size of 12 μm were successfully prepared with curing by heat and foaming by supercritical CO_2 as a green blowing agent. The microcellular silicone rubber foams exhibited a well-defined cell structure and a uniform cell size distribution. The crosslinking and foaming of silicone rubber was carried out separately. After foaming, the silicone rubber foam was cross-linked again to stabilize the foam structure and further improve its mechanical properties. Foaming process of cross-linked silicone rubber should be designed carefully based on the viscoelastic properties because of its elastic volume recovery in the atmosphere. The basic crosslinking condition for small cell size and high cell density was obtained after investigating the rheological behavior during crosslinking.

Keywords: Silicone Rubber, Crosslinking Reaction, Gel Point, Supercritical Carbon Dioxide, Foaming

INTRODUCTION

A supercritical fluid is a substance for which both pressure and temperature are above the critical values (Fig. 1 [1]) and displays intermediate properties between those of a liquid and a gas [2-4]. The liquid-like density of a supercritical fluid makes it have a much higher solubility power compared to gas. Moreover, its gas-like viscosity provides very high rate of diffusion. As an excellent solvent or plasticizer, a supercritical fluid has been used in many applications of polymer processing such as polymer synthesis, polymer blending and composites, polymer modification, and polymer foaming [4-7].

Silicone materials have many applications from aerospace applications to medical devices [8-11] due to their low toxicity, inertness, good blood compatibility, flexibility, reliability, and good thermal, oxidative, mechanical stabilities over a wide range of temperature and humidity [11-14]. Silicone rubber is a thermoset elastomer that is solidified exothermally by a cross-linking reaction called curing [15]. There are three kinds of curing: addition curing, peroxide-initiated curing, and condensation curing. The cure of liquid silicone rubber is almost exclusively carried out with a platinum-catalyzed hydrosilyation reaction, which does not generate by-products [16]. If platinum-olefin complexes are used, curing will take place at room temperature. Platinum complexes containing nitrogen are used for effecting addition curing at elevated temperatures. The silicone rubber studied in this work is a thermally curable, addition-curing, two-part, liquid silicone rubber, and is depicted in Scheme 1. A hydrosilylation reaction occurs when sufficient heat is applied (Fig. 2).

A common technique for the foaming of rubbers consists of crosslinking and foaming. Rubbers are usually cross-linked by con-

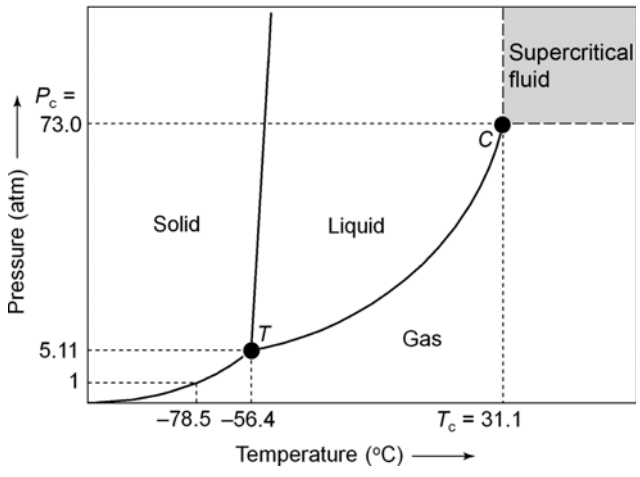

Fig. 1. Phase diagram of carbon dioxide [28].

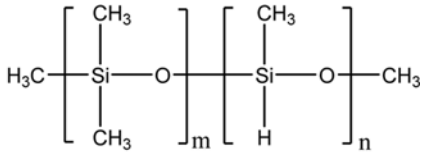

Methylhydrogen, polydimethylsiloxane

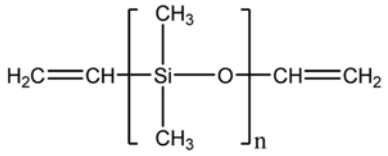

Vinyl terminated polydimethylsiloxane

Scheme 1. Chemical structure of materials used in this study.

†To whom correspondence should be addressed.
E-mail: sangmooklee@dankook.ac.kr, s_mlee@naver.com

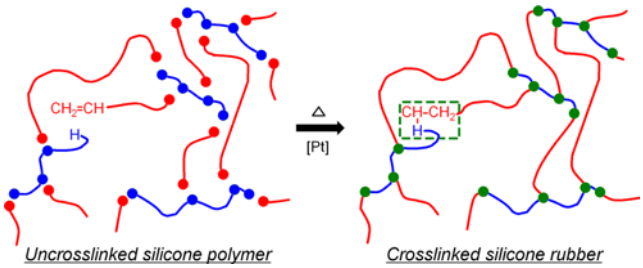

Fig. 2. Addition cure mechanism of silicone rubber (red dot: -CH=CH_2; blue dot: -H; green dot: -CH_2-CH_2-).

ventional chemical methods and expanded through the decomposition of chemical blowing agent. In closed-cell foam, the gas is dispersed as gas bubbles and the rubber matrix forms a continuous phase [17-21]. The balance of cell growth and crosslinking progress is important in foaming of rubbers and is crucial to obtain rubber foams with excellent properties [22]. The foams with fine cell size less than 10 μm by using physical blowing agents (e.g., carbon dioxide and nitrogen) is called microcellular polymer foams [23], which have many applications including thermal and electrical insulation, catalyst supports, membranes and drug delivery rate control [24].

In this study, carbon dioxide and silicone rubber were used as a physical blowing agent and a matrix polymer, respectively. During cure of silicone rubber, the rheological change was measured and the cure degree was evaluated by the storage modulus. The effects of cure degree before foaming and processing condition on the final cell size of foamed silicone rubber were investigated.

EXPERIMENTAL

1. Materials

Commercially available silicone reactants were kindly supplied by Bluestar Silicones as a two part system (Silbione LSR 4330) with silica filler (27 wt%). The crosslinking takes place by the addition-cure reaction of vinyl endblocked groups with Si-H groups. The chemical structures of vinyl terminated poly(dimethyl siloxane) and methylhydrogen poly(dimethyl siloxane) used are shown in Scheme 1. Carbon dioxide (Daedong gas tech Co. 99.8%) as the blowing agent was used as received without further purification.

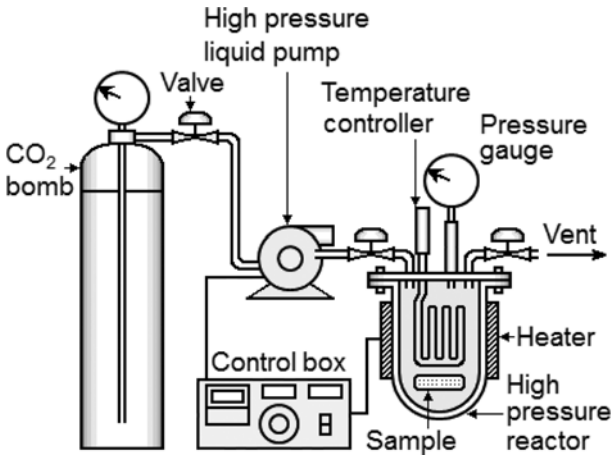

Fig. 3. Schematic diagram of the system used to generate silicone rubber foams in supercritical carbon dioxide.

2. Sample Preparation and Foaming

Two parts of silicone reactants were thoroughly mixed in a beaker by mechanical stirrer. Then the mixture was cast into a mold and degassed in an oven at room temperature under vacuum overnight. A schematic diagram of the experimental apparatus used in this work is shown in Fig. 3. Before foaming, pre-curing was done to give the molded samples proper elasticity and mechanical property at 80-180 °C for 15-60 minutes using convection oven. Carbon dioxide was pumped into sorption vessel, which was preloaded with several test pieces of silicone rubber. The vessel was equipped with a heating jacket and a temperature controller. The pressure in the vessel was adjusted through pressure control knob in the pump and displayed on the window of the control box. First, the vessel was flushed with low-pressure carbon dioxide from the gas cylinder for about 5 minutes and then charged with the carbon dioxide up to a desired saturated pressure at a constant temperature. A liquid pump was used for the pressurization to supercritical condition. After enough time for saturation of the test pieces, the pressure in the vessel was then released to the atmospheric pressure as quickly as possible. The test pieces were immediately taken out of the vessel after depressurization. It took at least 2 minutes to take them out. After foaming, post-curing was done to keep the cell finally at 200 °C for 20 minutes using convection oven. A schematic of foaming strategy utilized in this study is presented in Fig. 4.

3. Differential Scanning Calorimetry

To investigate the proper curing condition, differential scanning calorimetry (DSC) was performed on DSC Q-series (TA, U. S. A.). The silicone rubber mixture of about 8 mg was heated from 50 to 150 °C at a heating rate of 10 °C/min in flowing nitrogen gas.

4. Rheological Measurement

Storage modulus, loss modulus, and complex viscosity of the silicone rubber mixture were measured using an AR-G2 rotational rheometer (TA Instruments, Inc.) on which a 25 mm diameter parallel plate with a gap size of 1.0 mm was mounted. The frequency was

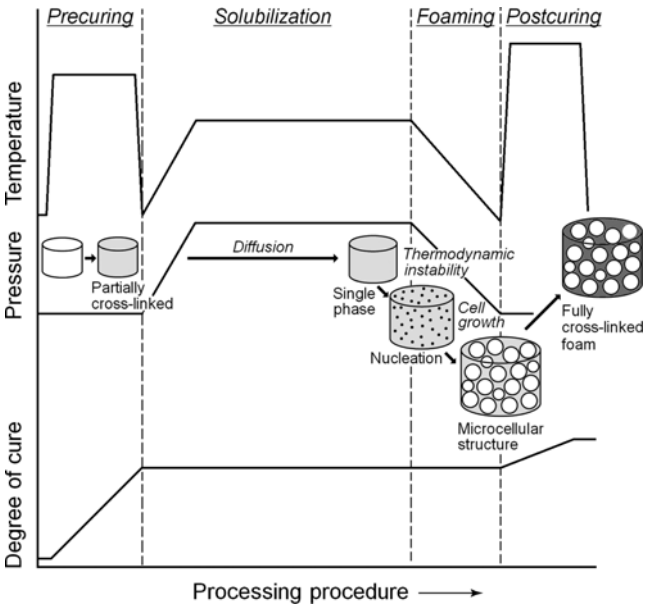

Fig. 4. Schematic of the foaming strategy utilized in this study.

fixed at 50 rad/s and the applied strain was 5% which was enough to ensure a linear viscoelastic response of the polymers. Measurements were done at various temperatures (70, 75, 80, 85, 90, and 95 °C) under nitrogen atmosphere.

5. Morphology

The fractured surface morphologies were observed using a scanning electron microscope (SEM, Hitachi S-2500, 25 kV). A part of the foamed samples were cryo-fractured and sputter-coated with gold before viewing under the microscope.

RESULTS AND DISCUSSION

Dynamic DSC scan was carried out at 10 °C/min to determine the basic curing behavior of silicone rubber, as shown in Fig. 5. An exothermal peak was observed about 109 °C and below this temperature isothermal rheological measurements were performed. During crosslinking, the change of viscosities was measured (Fig. 6). The complex viscosities increased with increasing time and did so more rapidly with increasing temperature.

In Fig. 7, the change of tan delta during curing reaction of silicone rubber is plotted versus time for various temperatures and the gel time is re-plotted versus 1000/T. An important mark during crosslinking is the so-called gel point, which characterizes the state when a penetrating network of cross-linked molecules comes into exist-

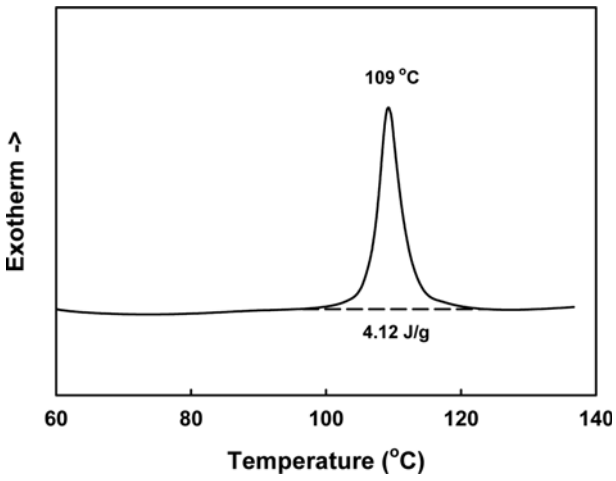

Fig. 5. Dynamic DSC curve of silicone rubber at 10 °C/min.

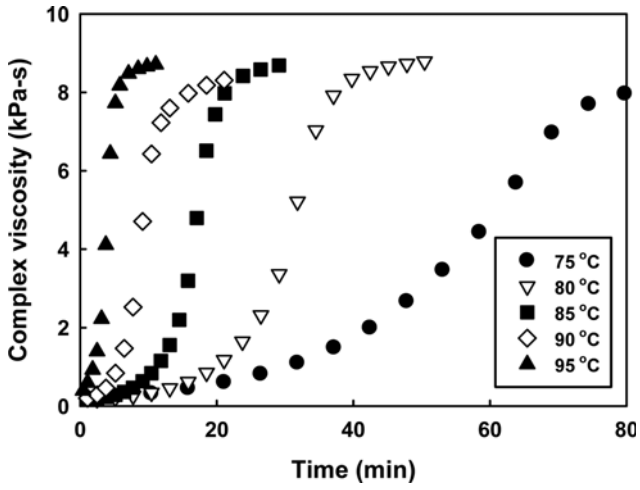

Fig. 6. Complex viscosities for curing of silicone rubber at various temperatures.

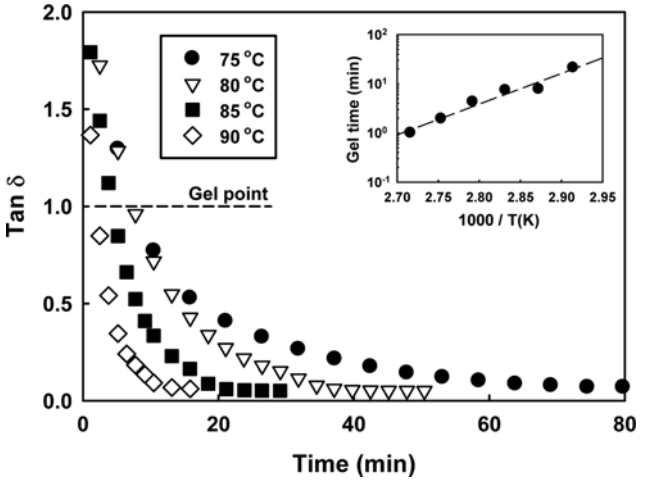

Fig. 7. Tan delta and gel time for curing of silicone rubber at various temperatures.

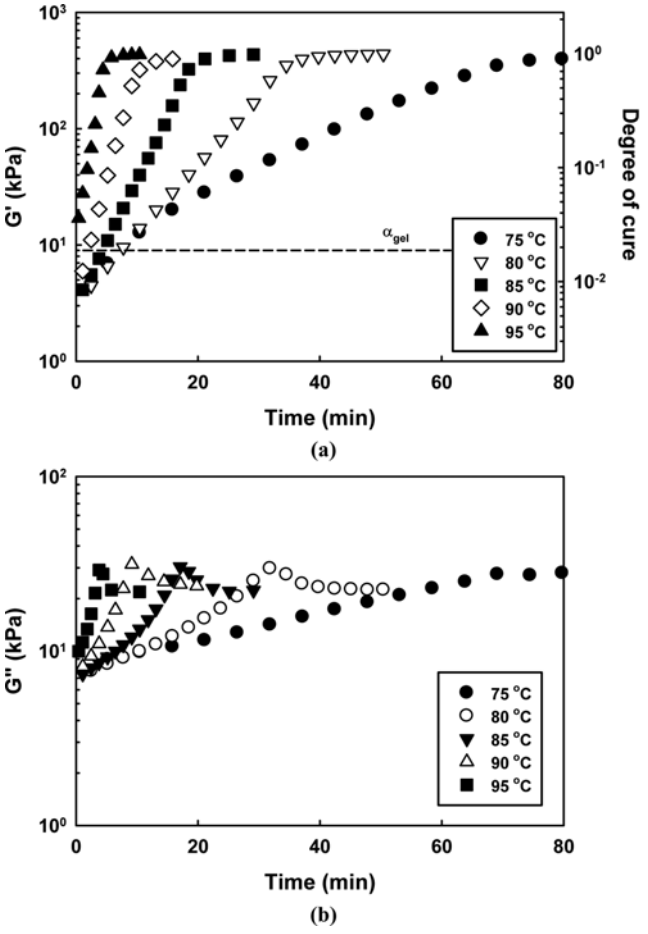

Fig. 8. Shear storage modulus (a) and shear loss modulus (b) for curing of silicone rubber at various temperatures, respectively.

ence for the first time. In real processing, knowing the gel time of cross-linkable material is very important because the processing after gel time is almost impossible due to its high viscosity. The gel point can be obtained from the crossover of G′ and G″, i.e., tan delta= 1, which denotes the transition from a viscoelastic fluid to a viscoelastic solid by the sufficient entanglements of polymer chains [25]. The gel time obtained from tan delta curves obeyed the Arrhenius equation (Fig. 7).

Fig. 8 shows the shear storage modulus change and the shear loss modulus change during crosslinking. From the rheological viewpoint, degree of cure may be defined by [26]:

$$\alpha = \frac{G'(t) - G'(0)}{G'(\infty) - G'(0)} \quad (1)$$

where G′(0), G′(t), and G′(∞) are the shear storage modulus at time 0, at time t, and at t→∞, respectively. This equation implies the ratio of the amount of macro-radicals reacted before time t to the amount of macro-radicals formed in the whole reaction.

The degree of cure obtained by Eq. (1) is also shown in Fig. 8 with the shear storage modulus. The values of degree of cure at time zero are not zero, which shows the cure during the preparation time before starting the test. However, the values are so small and those reactions have negligible influence on the following reaction and calculations. We considered the value of storage modulus at time zero as zero. The degree of cure at the gel point can be obtained from Fig. 7 and Fig. 8(a) as the procedure. First, the gel time was found from the time at tan δ=1 in Fig. 7 (large graph). Next, the storage modulus at gel point was obtained from crossover of the gel time and the storage modulus curve at a given curing temperature in Fig. 8(a). Finally, the degree of cure at gel point could be determined by reading the value of the right axis in Fig. 8(a) corresponding to the storage modulus obtained from the second step. The degree of cure at gel point and the value of G′ are close to 0.02 and 9 kPa regardless of curing temperatures, respectively, which might imply that the microstructures of the cross-linked silicone rubber are nearly the same.

Assuming the conversion of reactive species at the gel point to be independent of temperature, a plot of ln t_{gel} versus 1/T should then produce a line of slope E_a/R as shown in Fig. 7 (small graph).

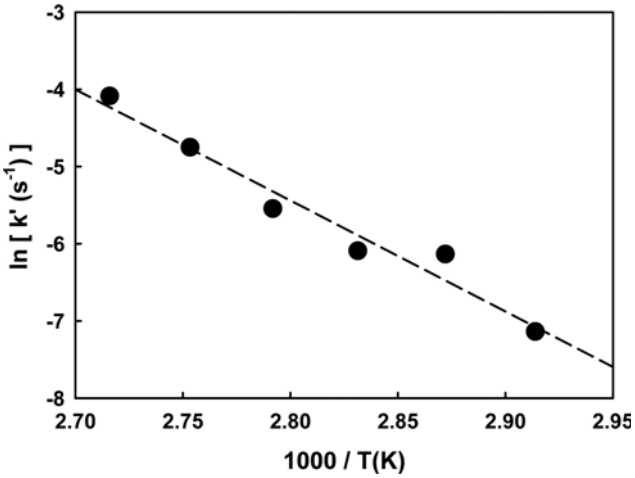

Fig. 9. Reaction rate constants, ln k′[=ln(1/t_{gel})] versus 1000/T.

The reaction rate constant, k′=1/t_{gel} was calculated. Least squares linear regression of ln k′ vs. 1/T to fit the equation yields the expression (Fig. 9).

$$k' = k'_{\infty}\exp\left(\frac{-\Delta E_k'}{T}\right) \text{ and } k' = 1.340\times10^{15}\exp\left(\frac{-1.438\times10^4}{T}\right) \quad (2)$$

The reaction rate activation energy obtained using DSC [27] is nearly same as the activation energy obtained from the gel time data.

$$k = 1.118\times10^{15}\exp\left(\frac{-1.401\times10^4}{T}\right) \quad (3)$$

Viscosity profiles for a given resin can be superimposed by shifts along the time and logarithmic viscosity axes. The resulting viscosity master curve is presented in Fig. 10. The amount of the shift, using one of the lowest temperature runs as a reference, is the shift factor (logarithm of the shift multipliers), defined as follows:

$$\text{Time shift factor: } a_t \equiv t_{gel,\,ref}/t_{gel} \quad (4)$$

$$\text{Viscosity shift factor: } a_\eta \equiv \eta_{gel,\,ref}/\eta_{gel} \quad (5)$$

where reference temperature was 70 °C.

The rate of change of the shift factor with temperature gives viscous flow activation energy. The shift multipliers, a_t and a_η, have been calculated and then fitted to Arrhenius equations as follows:

$$a_t = 1.596\times10^{18}\exp\left(\frac{-1.438\times10^4}{T}\right) \quad (6)$$

$$a_\eta = 2.844\exp\left(\frac{-3.605\times10^2}{T}\right) \quad (7)$$

Interpolations within the temperature range studied are accurate to

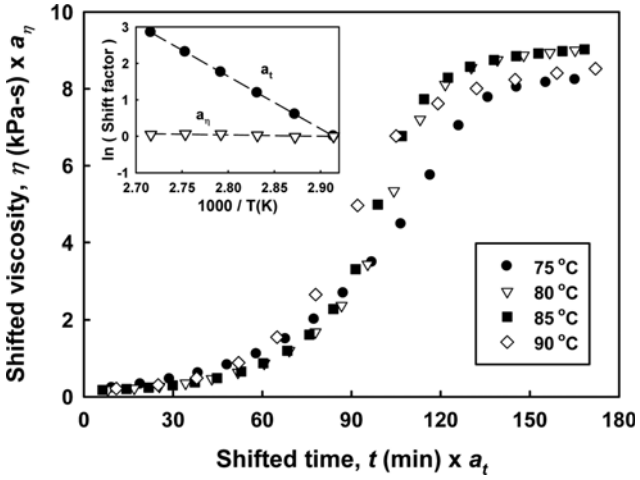

Fig. 10. Viscosity master curve for curing of silicone rubber.

Table 1. Effect of processing condition and degree of cure on the cell size

	Pre-curing condition	Foaming condition	Degree of cure	Cell size (mm)
Case I	80 °C/24 min	52 °C/2000 psi/2 hr	0.2	220
Case II	80 °C/30 min	52 °C/2000 psi/2 hr	0.5	12
Case III	180 °C/20 min	52 °C/2000 psi/2 hr	1.0	305

within 10 percent. Extrapolations outside the temperature range studies could lead to large errors because reaction mechanisms or physical state could change with temperature. This master plot can be used to determine the viscosities of silicone rubber from known times and temperatures. Even at unknown times and temperatures, the viscosities during curing reaction can be obtained by simply applying a shift operation.

Table 1 summarizes the results for the effect of processing condition and degree of cure on the cell size. The curing conditions for a certain degree of cure (0.2, 0.5, and 1.0) in Table 1 were determined from the time and temperature corresponding to the degree of cure in Fig. 8(a). Microcellular silicone rubber foams are different from thermoplastic foams because they exhibit obvious volume shrinkage in the atmosphere, which are caused from the elasticity of the polymer matrix. CO_2 diffusivity was also an important governing factor in the cell growth process. Fig. 11 shows the obtained morphologies of foamed silicone rubber, which reveal the existence of optimum condition in microcellular foaming of silicone rubber. When the degree of cure was 0.2, the cell size was large, about 220 μm, and the cell density was moderate, as shown in Fig. 11(a). It could be observed even open cells. This might be due to the fact that the elastic force of the silicone rubber was not high enough yet to hold cells stable. As the degree of cure was increased to 0.5, finer uniform cell size of 12 μm with well defined, closed cell structure, and high cell density was obtained as shown in Fig. 11(b). At this condition, it is believed that cell growth and crosslinking are in balance. When degree of cure was increased further, i.e., fully cured, poor foaming occurred as shown in Fig. 11(c). It is thought that high cure degree increased storage modulus and viscosity of the silicone rubber matrix, decreased the CO_2 solubility and diffusivity, limited cell growth and resulted in poor cell density and cell size distribution. It corresponds to the region III in the work of Shimbo et al. [28]. They observed that the cells could not generate and grow in fully vulcanized rubber because of its high elasticity. These results show that fine microcellular silicone rubber foam can be achieved by optimizing the cure condition carefully after investigating the viscoelastic behavior during crosslinking.

The average cell size was obtained by number-averaging the diameter of all cells in the SEM micrograph, and the cell density, defined as the number of cells per unit volume of the foam, was calculated from SEM micrographs using the method proposed by Kumar and Suh [29]. In case III, however, the cell size was obtained by rough number-average of several SEM micrographs because only a few cells could be found. Fig. 12 shows the relationship between average cell size, cell density and cure degree of foamed silicone rubber. Case II (degree of cure 0.5) showed the smallest cell size and the

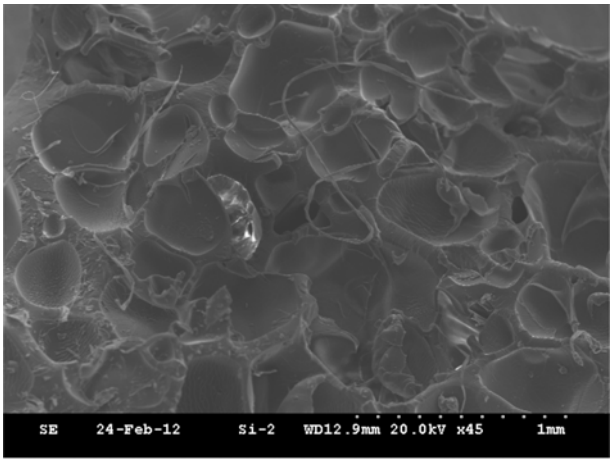

(a) Cass I, $\alpha = 0.2$

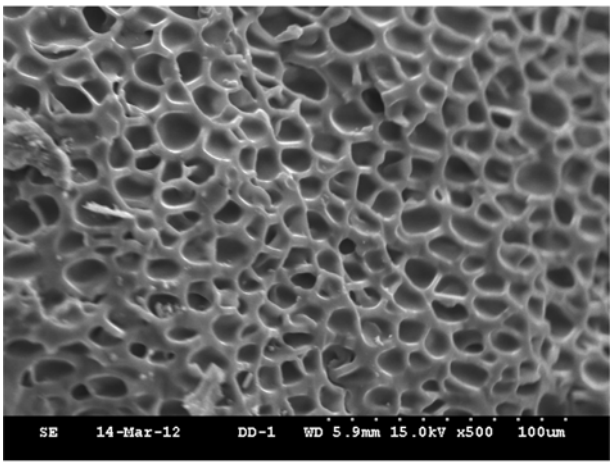

(b) Cass II, $\alpha = 0.5$

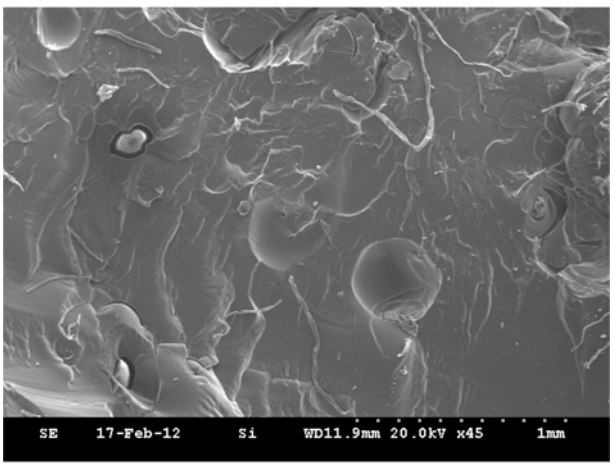

(c) Cass III, $\alpha = 1.0$

Fig. 11. SEM micrographs of foamed silicone rubber at different degree of cure.

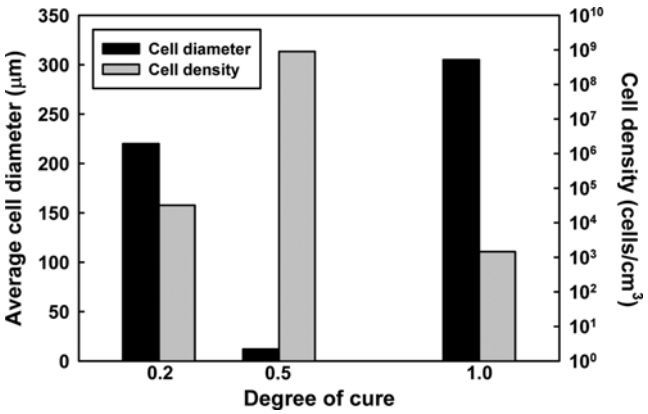

Fig. 12. Average cell size and cell density as a function of degree of cure.

highest cell density among three cases tested in this work.

CONCLUSIONS

The crosslinking and foaming of silicone rubber was carried out separately. After foaming, the silicone rubber foam was fully cured to stabilize the foam structure and further improve its mechanical properties. Different process conditions were applied to determine the foaming behaviors of the silicone rubber and the effect of cure degree and saturation condition on the cell growth. The foam morphology could be controlled by the curing condition. Increasing cure degree produced denser foams with smaller cell sizes in the range of low cure degree (<0.5). Fully cured sample showed the largest cell size and a very poor cell density with large cell sizes. It might be due to volume shrinkage caused from the elasticity of the silicone rubber matrix. The CO_2 saturation condition had not nearly an influence on the morphology of the foam in our work scope. In this work, a proper cure degree seemed to be about 0.5 of cure degree among the cases tested. At this condition, the microcellular foamed samples with a cell size of 12 μm were successfully obtained and exhibited a well-defined cell structure, a high cell density and a uniform cell size distribution. These basic works demonstrate the feasibility of producing microcellular silicone rubber and allow for a control of the foam morphology, enabling a wide range of specialty applications, such as electric and medical devices by thermal curing and subsequent foaming with a supercritical carbon dioxide as a green blowing agent.

REFERENCES

1. W. Leitner, *Nature*, **405**, 129 (2000).
2. S. C. Tucker, *Chem. Rev.*, **99**, 391 (1999).
3. O. Kajimoto, *Chem. Rev.*, **99**, 355 (1999).
4. M. A. McHugh and V. J. Krukonis, *Supercritical fluid extraction*, Butterworth-Heinemann (1994).
5. S. Alsoy and J. L. Duda, *Chem. Eng. Technol.*, **22**, 971 (1999).
6. J. L. Kendall, D. A. Canelas, J. L. Young and J. M. de Simone, *Chem. Rev.*, **99**, 543 (1999).
7. D. L. Tomasko, H. Li, D. Liu, X. Han, M. J. Wingert, L. J. Lee and K. W. Koelling, *Ind. Eng. Chem. Res.*, **42**, 6431 (2003).
8. R. Hernandez, J. Weksler, A. Padsalgikar and J. Runt, *Macromolecules*, **40**, 5441 (2007).
9. I. V. Yannas and J. F. Burke, *J. Biomed. Mater. Res.*, **14**, 65 (1980).
10. F. Abbasi, H. Mirzadeh and M. Simjoo, *J. Biomater. Aci. Polym. Ed.*, **17**, 341 (2006).
11. Z. Gao, J. S. Nahrup, J. E. Mark and A. Sakr, *J. Appl. Polym. Sci.*, **96**, 494 (2005).
12. R. W. Hergenrother, Y. Xue-Hai and S. L. Cooper, *Biomaterials*, **15**, 635 (1994).
13. Y. B. Kim, D. Cho and W. H. Park, *J. Appl. Polym. Sci.*, **116**, 449 (2010).
14. R. Hernandez, J. Weksler, A. Padsalgikar and J. Runt, *J. Biomed. Mater. Res.*, **87A**, 546 (2008).
15. R. J. Young and P. A. Lowell, *Introduction to polymers*, 2nd Ed., Chapman and Hall, UK (1991).
16. L. Lopez, A. Cogrove, J. P. Hernandez-Ortiz and T. A. Osswald, *Polym. Eng. Sci.*, **47**, 675 (2007).
17. B. Kamarudin, M. Hiroshi, E. Taro, Y. Fumio and M. Keizo, *Polym. Deg. Stab.*, **62**, 551 (1998).
18. Z. Ghazali, A. F. Johnson and K. Z. Dahlan, *Rad. Phys. Chem.*, **55**, 73 (1999).
19. J. Heiner, B. Stenberg and M. Persson, *Polym. Testing*, **22**, 253 (2003).
20. R. L. Warley, D. L. Feke and I. Manas-Zloczower, *J. Appl. Polym. Sci.*, **97**, 1504 (2005).
21. G. Baquey, L. Moine, O. Babot, M. Degueil and B. Maillard, *Polymer*, **46**, 6283 (2005).
22. H. Kawashima and M. Shimbo, *Cellular Polymers*, **22**, 175 (2003).
23. J. E. Martini, N. P. Suh and F. A. Waldman, US Patent, 4,473,665 (1984).
24. J. S. Colton and N. P. Suh, *Polym. Eng. Sci.*, **27**, 500 (1987).
25. C. Y. M. Tung and P. J. Dynes, *J. Appl. Polym. Sci.*, **27**, 569 (1982).
26. A. Y. Malkin, S. G. Kulichikhin, M. L. Kerber, I. Y. Gorbunova and E. A. Murashova, *Polym. Eng. Sci.*, **37**, 1322 (1997).
27. I.-K. Hong and S. Lee, *J. Ind. Eng. Chem.*, **19**, 42 (2013).
28. M. Shimbo, T. Nomura, K. Muratani and K. Fukumura, *The 3rd international conference on axiomatic design*, Seoul, ICAD-2004-25 (2004).
29. V. Kumar and N. P. Suh, *Polym. Eng. Sci.*, **30**, 1323 (1990).